Author(s): D. Lepilin, A. Laurén, J. Uusitalo, H. Fritze, R. Laiho, B. Kimura, and E.-S. Tuittila

Title: Response of vegetation and soil biological properties to soil deformation in logging trails of drained boreal peatland forests

Year: 2022

Version: Published version

Please cite the original version:

D. Lepilin, A. Laurén, J. Uusitalo, H. Fritze, R. Laiho, B. Kimura, and E.-S. Tuittila. Response of vegetation and soil biological properties to soil deformation in logging trails of drained boreal peatland forests. Canadian Journal of Forest Research. 52(4): 511-526. https://doi.org/10.1139/cjfr-2021-0176.

Canadian Science Publishing

ARTICLE

Response of vegetation and soil biological properties to soil deformation in logging trails of drained boreal peatland forests

D. Lepilin, A. Laurén, J. Uusitalo, H. Fritze, R. Laiho, B. Kimura, and E.-S. Tuittila

Abstract: In the boreal region, peatland forests are a significant resource of timber. Under pressure from a growing bioeconomy and climate change, timber harvesting is increasingly occurring over unfrozen soils. This is likely to cause disturbance in the soil biogeochemistry. We studied the impact of machinery-induced soil disturbance on the vegetation, microbes, and soil biogeochemistry of drained boreal peatland forests caused by machinery traffic during thinning operations. To assess potential recovery, we sampled six sites that ranged in time since thinning from a few months to 15 years. Soil disturbance directly decreased moss biomass and led to an increase in sedge cover and a decrease in root production. Moreover, soil CO_2 production potential, and soil CO_2 and CH_4 concentrations were greater in recently disturbed areas than in the control areas. In contrast, CO_2 and CH_4 emissions, microbial biomass and structure, and the decomposition rate of cellulose appeared to be uncoupled and did not show signs of impact. While the impacted properties varied in their rate of recovery, they all fully recovered within 15 years covered by our chronosequence study. Conclusively, drained boreal peatlands appeared to have high biological resilience to soil disturbance caused by forest machinery during thinning operations.

Key words: peat, drained peatlands, harvesting, PLFA, microbial biomass, roots, decomposition, soil CO_2, CH_4 and N_2O concentrations, soil CO_2 and CH_4 emissions.

Résumé : En région boréale, les forêts de tourbière constituent une importante ressource en bois. Soumise à la pression d'une bioéconomie croissante et du changement climatique, la récolte de bois s'étend de plus en plus sur des sols dégelés. Cela risque de perturber la biogéochimie du sol. Nous avons étudié l'impact de la perturbation du sol causée par la machinerie sur la végétation, les microorganismes et la biogéochimie du sol dans les forêts de tourbière boréale drainée due à la circulation de la machinerie lors des opérations d'éclaircie. Afin d'évaluer le potentiel de récupération, nous avons échantillonné six stations où le temps écoulé depuis l'éclaircie variait de quelques mois à 15 ans. La perturbation du sol a directement réduit la biomasse de la mousse et entraîné une augmentation du couvert de carex et une diminution de la production de racines. De plus, la production potentielle de dioxyde de carbone (CO_2) dans le sol et les concentrations de CO_2 et de méthane (CH_4) dans le sol étaient plus élevées dans les zones récemment perturbées que dans les zones témoins. Par contre, les émissions de CO_2 et de CH_4, la structure et la biomasse microbiennes ainsi que le taux de décomposition de la cellulose semblaient découplés et ne montraient aucun signe d'impact. Tandis que le taux de récupération des propriétés qui avaient été affectées variait, elles ont toutes récupéré pendant les 15 années couvertes par la chronoséquence que nous avons étudiée. Les tourbières boréales drainées semblent définitivement posséder une grande résilience biologique face aux perturbations du sol causées par la machinerie lors des opérations d'éclaircie. [Traduit par la Rédaction]

Mots-clés : tourbe, tourbières drainées, récolte, acides gras phospholipidiques (PLFA), biomasse microbienne, racines, décomposition, concentrations de CO_2, de CH_4 et d'oxyde de diazote (N_2O) dans le sol, émissions de CO_2 et de CH_4 provenant du sol.

1. Introduction

Forested peatlands are widespread in the boreal zone; approximately 24% of the total boreal forest area is classified as peatlands (Wieder et al. 2006). A large portion of these forested peatlands (originally open or with a tree stand) has been drained to improve tree growth and support forestry. At present, the ecosystem services provided by peatlands, such as carbon storage and water regulation, are considered important, and therefore, there is an increasing call for conservation of pristine peatlands and restoration of previously drained peatlands. However, drained peatland forests in northern Europe still play a significant role in the economy, e.g., in Finland drained peatland forests account for 26% of all forest areas (Päivänen 2008).

Because of the low load-bearing capacity of peat, forest harvesting with heavy machinery in drained boreal peatlands is traditionally conducted during the cold winter months when the soil is frozen and has a greater resistance to disturbance. However, harvesting during unfrozen conditions is becoming more common due to climate warming and the increasing demand for

Received 16 June 2021. Accepted 22 November 2021.

D. Lepilin, A. Laurén, and E.-S. Tuittila. School of Forest Sciences, University of Eastern Finland, Joensuu, Finland.
J. Uusitalo.* Natural Resources Institute Finland (Luke), Parkano, Finland.
H. Fritze, R. Laiho, and B. Kimura.[†] Natural Resources Institute Finland (Luke), Helsinki, Finland.
Corresponding author: Dmitrii Lepilin (email: dmitrii.lepilin@uef.fi).
*Present address: Department of Forest Sciences, University of Helsinki, Helsinki, Finland.
[†]Present address: Faculty of Medicine and Health Technology, Tampere University, Tampere, Finland.

 Published at www.cdnsciencepub.com/cjfr on 13 December 2021.

wood within the burgeoning bioeconomy (Uusitalo and Ala-Ilomäki 2013). As found for both undrained and drained peatlands, traffic over unfrozen soil causes disturbance of the upper peat layer, manifesting as severe rutting, erosion, and change of peat physical properties (Groot 1987; Nugent et al. 2003; Lepilin et al. 2019). The share of disturbed area affected by traffic varies and largely depends on harvesting machinery used, and can cover 4%–24% of harvested sites (Bettinger et al. 1994; Eliasson 2005; Frey et al. 2009; Cudzik et al. 2017; Talbot et al. 2018). In Finland, almost all harvesting operations are fully mechanized with use of machines that commonly utilize trail spacing of 20 m with 4-m-wide logging trail. That corresponds to approximately 20% of logging trail cover. Given the large proportion of forest peatlands, these disturbances affect a significant area of the boreal zone.

The disturbance caused by harvesting primarily impacts peat physical properties, such as bulk density and water retention characteristics (Chow et al. 1992; Nugent et al. 2003; Lepilin et al. 2019). Changes in peat physical properties may then be reflected in both soil biological processes and plant community responses as found in undrained peatlands in Canada (Echiverri et al. 2020; Davidson et al. 2021). The effect on the biological processes is primarily due to the changed pore size distribution and decreased air-filled porosity, which further cause restriction of gas exchange. In general, a decrease in soil porosity restricts oxygen availability and, therefore, is likely to lead to an increase of CO_2 concentration in peat, which has previously been reported for mineral soils (Gaertig et al. 2002; Goutal et al. 2012). Severe reduction of soil diffusive transport is found to lead to accumulation of CO_2, which further restricts soil respiration. All these factors in turn have been found to limit root growth (Bodelier et al. 1996; Startsev and McNabb 2001) and microbial activity (Marshall 2000; Frey et al. 2009), and lead to changes in microbial communities and microbial biomass (Jordan et al. 2003; Li et al. 2004; Tan et al. 2005).

While research on the impact of forest harvesting on the soil biology of drained peatland forests is still lacking, recent research in Canada has revealed a drastic impact of seismic lines (exploration lines) used for resource extraction on the vegetation, soil properties, and biogeochemistry. Seismic line disturbances resemble in several respects harvesting-induced disturbances, and have been found to alter soil properties by increasing bulk density, volumetric water content, and rate of organic matter decomposition manifested in decreased organic matter content (Davidson et al. 2020). Additionally, seismic line disturbances were found to alter vegetation structure and phenology causing an earlier seasonal peak and a shift in vegetation composition to sedge and willow dominance with decreased moss abundance (Davidson et al. 2021). Deane et al. (2020) observed a shift from feather moss to *Sphagnum* moss dominance on seismic lines opposingly to the surrounding undisturbed forested peatland. There are also findings of vegetation succession towards undisturbed state following the initial disturbance. Echiverri et al. (2020) noted evident recovery of the understory community of extraction lines, with shrub and total understory cover similar to reference treed fens. Earlier, we found impacts on soil physical properties in drained peatland forests following harvesting similar to those found following construction of seismic lines in undrained peatlands in Canada (Lepilin et al. 2019). Our study also revealed recovery following initial disturbance in bulk density and pore size distribution. However, harvesting impacts on vegetation, soil biological activity, and biogeochemical cycling of drained peatland forests are yet to be assessed.

In this study, we quantified the response of plant community and soil biological properties to disturbance induced by forestry vehicles during forest thinning operations and evaluated their potential recovery from disturbance. To address those aims, we studied vegetation composition and biomass production, microbial biomass and phospholipid fatty acid (PLFA) profiles, carbon dioxide (CO_2) production potential, cellulose decomposition rate, greenhouse gas (GHG) emissions, and GHG soil concentrations in sites at different points in time (years) since thinning. Based on our earlier study (Lepilin et al. 2019) that showed initial disturbance in soil physical properties and following recovery within 15 years since harvesting operations, we hypothesized that the initial disturbance (*i*) affects the studied response variables and (*ii*) shows recovery similar to physical properties. Findings from mineral soils and undrained peatlands allow us to expect disturbance to cause increase in *Sphagnum* cover and decrease in dwarf shrubs, alteration in microbial community structure, decrease in microbial biomass, CO_2 production potential, cellulose decomposition rate, root production, and increase in methane production and emissions.

2. Materials and methods

2.1. Experimental layout

The study was conducted on six forestry-drained peatlands located in southern Finland (Table 1). Selected sites shared similar peat and stand characteristics: mean annual temperature (4–5 °C), mean temperature of the coldest and warmest month (January and July: −6.2–6.2 °C and 15.2–16.2 °C, respectively); and the dominant tree species: Scots pine (*Pinus sylvestris* L.). Physical properties such as bulk density (mean 105 $kg \cdot m^{-3}$), field capacity (mean 0.42 $m^3 \cdot m^{-3}$ at 10 kPa), von Post, loss on ignition, and water retention characteristic of peat soil, unaffected by harvesting machinery traffic, were similar for all study sites (Lepilin et al. 2019) (Table 1). The understory vegetation was dominated by forest and peatland dwarf shrubs. According to the Finnish classification of drained peatland forests (Laine and Vasander 2008), the sites represented Ptkg (*Vaccinium vitis-idaea*) and Vatkg (dwarf shrub) types. The drainage of the sites was performed during 1960s–1970s, and the ditches were cleaned 20 years later. All sites were subjected to harvesting operations (thinning) only once before sampling.

To assess the recovery from harvesting, i.e., the temporal change in soil properties since harvesting, we grouped the study sites into three age classes (AC1, AC2, and AC3). Each age class corresponded to the time elapsed after thinning and formed the following chronosequence: AC1 sites were thinned in July 2013, AC2 sites were thinned in August 2009 and August 2010, AC3 sites were thinned in July 1999. As field sampling and measurements were carried out in 2013–2014, the AC1 sites represent conditions immediately after thinning, while AC2 corresponds to 4–5 years and AC3 14–15 years after thinning (Fig. 1).

Study plots representing three disturbance classes (DC0, DC1, and DC2), based on rut depth, were randomly chosen in each study site. A rut depth of 0.2 m was used as a threshold for DC1 (rut depth < 0.2 m) and DC2 (rut depth > 0.2 m), as it is the maximum acceptable trail depth according to Finnish forest management recommendations (Vanhatalo et al. 2015). DC0 represented plots unaffected by machine traffic. The disturbance classes DC1 and DC2 included three plots per study site while disturbance class DC0 included six plots per study site. In total, the study included 72 individual plots. Plot size was approx. 1 m^2.

The response of peat physical properties to thinnings previously reported by Lepilin et al. (2019) used the same chronosequence approach and plots classified accordingly in age and disturbance classes. The main changes were an increase of soil bulk density (up to 190 $kg \cdot m^{-3}$) and field capacity (0.67 $m^3 \cdot m^{-3}$ at 10 kPa), as well as a decrease of total porosity and changes in pore structure reflected in water retention characteristic (Lepilin et al. 2019). The study also found the recovery of physical properties within 15 years after disturbance (Table 2).

2.2. Vegetation

To evaluate changes in the vegetation after disturbance, we assessed vegetation composition and quantified living moss biomass and the root production rate in each study plot. In July 2014, vegetation composition was assessed by estimating the cover of each vascular plant and moss species using a scale within

Table 1. Characteristics of the study sites.

Site	Age class	Average peat depth (cm)	Coordinates (latitude; longitude)	Harvesting machinery	Years after thinning	Mean von Post	LOI (%)	DBH (cm)	Volume of trees ($m^3 \cdot ha^{-1}$)	Mean estimated cover (%) of: *Sphagnum* mosses	Other mosses	Dwarf shrubs	Forbs	Sedges
Varsapuro	AC1	176	62.60928; 24.62267	8-wheel Ponsse Fox, 10-wheel Ponsse Buffalo	<1	3.8±0.7	94.4±2.2	16	160	35±37	15±17	15±10	2±4	1±1
Permisuo	AC1	98	62.20058; 24.52608	ProSilva 910, ProSilva 15-4ST	<1	3.9±0.8	96.4±1.7	18	190	32±40	34±27	25±6	4±8	1±1
Vuorijärven	AC2	101	61.82745; 24.3169	J.Deere 1070D, J.Deere 810E	4	3.7±0.8	97.9±0.8	15	184	0±0	50±22	21±10	8±12	1±2
Mustakeidas	AC2	202	61.76302; 22.64543	J.Deere 1270D, J.Deere 1110D, ProSilva 15-4ST	5	3.8±0.6	97.7±1.4	16	130	16±39	48±33	9±9	11±9	1±2
Isoneva	AC3	53	61.9425; 22.94602	NA	14	4.0±0.9	98.1±0.9	21 (13)[a]	179 (50)[a]	0±0	42±26	17±5	12±27	4±7
Vehkasuo	AC3	108	61.7848; 23.99262	NA	15	3.8±0.6	96.6±0.8	16 (10)[a]	90 (27)[a]	25±38	49±37	15±14	5±4	5±7

Note: von Post, peat decomposition stage in the top 10 cm layer according to the von Post scale. LOI, peat loss on ignition (4 h at 600 °C); adapted from Lepilin et al. (2019). DBH, diameter at breast height. NA, information not available. ± standard deviation. Mean total cover of *Sphagnum* mosses, other mosses, dwarf shrubs, forbs, and sedges are given for the control plots.

[a]Stand characteristics were measured 6–9 years after thinning operation. Values for the removed trees (given in the parentheses) were estimated from stumps remaining at the moment of the measurements.

a circular frame (diameter 0.31 m, area approx. 754 cm^2) located in the center of the plot similarly to Kokkonen et al. (2019). The same person (Janne Sormunen) carried out all estimations. For species names we followed The Plant List (2013). Moss biomass was estimated by collecting 100 cm^2 samples of living moss in September 2013 and weighing after oven-drying at 60 °C for 48 h. The distinction between living and dead moss was based on the green pigment and was always carried out by the same person (Dmitrii Lepilin) to minimize personal error. The root production rate was determined using root ingrowth cores (Laiho et al. 2014) installed in October 2013 and collected 1 year later in October 2014. Ingrowth cores were cylindrically shaped mesh bags (diameter: 3 cm; length: 30 cm) filled with commercial unfertilized *Sphagnum* peat material. The roots ingrown into the mesh bags were extracted in the laboratory, and the annual root production was calculated as the mass of oven-dried (at 60 °C) roots per area. Root production was determined for two depths (0–10 cm; 10–20 cm).

2.3. Microbiology

The possible effect of machinery-induced peat disturbance on microbial carbon and community composition was evaluated with the chloroform fumigation–extraction (FE) method (Vance et al. 1987; Voroney et al. 2008) and phospholipid fatty acid (PLFA) analysis (e.g., Pennanen et al. 1999), which allow quantitative and qualitative estimation of the microbial biomass. For these analyses, we collected 72 independent peat samples (6 cm × 6 cm × 10 cm; 24 per each age class) in August 2013. The peat used in the analyses was cleaned of living roots and other non-peat materials. The dry mass was estimated from subsamples dried at 105 °C.

Microbial biomass carbon (C_{mic}) was determined by the FE method. Three fumigated and three non-fumigated replicates of each peat sample (72 independent samples × 2 fumigated/non-fumigated × 3 replicates = 432) were used. Twenty-millilitre samples of fresh peat were fumigated with alcohol-free $CHCl_3$ for 24 h. Afterwards, the fumigated and non-fumigated samples were extracted with 80 mL of 0.5 $mol \cdot L^{-1}$ K_2SO_4; and the filtered extracts were analyzed for dissolved organic carbon using a total organic carbon analyzer. Then, C_{mic} was calculated as the difference between the organic carbon extracted from the fumigated (C_F) and non-fumigated (C_{UF}) soil samples (eq. 1).

$$(1) \qquad C_{mic} = \frac{(C_F - C_{UF})}{k_{EC}}$$

where k_{EC} = 0.378 is the coefficient of extraction efficiency (Vance et al. 1987).

To describe the microbial community composition, we performed PLFA analysis using 2.5 g of fresh peat from each of the 72 samples. In total, 43 different PLFAs were identified from each sample and were used to determine the community composition and to calculate the microbial biomass indicators $PLFA_{total}$, $PLFA_{bact}$, and $PLFA_{fung}$ (Pennanen et al. 1999).

2.4. Biological activity

The biological activity of the peat soil was described by the potential CO_2 production rate measured under laboratory conditions (Peltoniemi et al. 2015), and by determining the in situ decomposition rate of cellulose strips (Lähde 1974). The 10-cm-wide strips were oven-dried (24 h at 105 °C), weighed and placed in separate nylon net bags (1 mm mesh size). In the field, the bags were inserted into the peat at each plot covering following depths: 0–5, 5–10, 10–20, and 20–30 cm. A total of 72 bags were inserted into the peat and marked with wooden poles. The bags were inserted in September 2013 and collected in September 2014. The collected cellulose strips were washed with water, oven-dried, and weighed. The corresponding mass loss (%) was considered as the decomposition rate over 1 year.

Fig. 1. Typical logging trails representing the three different age classes: (*a*) age class 1 (<1 year since logging), (*b*) age class 2 (4–5 years since logging), (*c*) age class 3 (14–15 years since logging) in the chronosequence. [Colour online.]

Table 2. Mean peat bulk density (ρ) and field capacity, by age and disturbance classes.

Age class	Disturbance class	ρ (kg·m^{-3})	Field capacity at 10 kPa (m^3·m^{-3})
AC1	DC0	113±26	0.42
AC1	DC1	190±32	0.64
AC1	DC2	168±29	0.67
AC2	DC0	104±18	0.42
AC2	DC1	137±18	0.53
AC2	DC2	97±7	0.56
AC3	DC0	102±15	0.42
AC3	DC1	118±19	0.56
AC3	DC2	115±19	0.49

Note: ± standard deviation. Age classes: AC1, <1 year since thinning; AC2, 4–5 years since thinning; AC3, 14–15 years since thinning. Disturbance classes: DC0, undisturbed; DC1, rut depth <0.2 m; DC2, rut depth >0.2 m. Adapted from Lepilin et al. (2019).

Peat samples for the potential CO_2 production measurements (Peltoniemi et al. 2015) were collected in August 2013 from each plot. Then, 1 g of each sample at fresh field moisture was incubated in a 100 mL glass bottle at 18 °C for 2 weeks. The CO_2 evolved over 72 h (μL·g^{-1} peat dry mass) was measured five times with thorough aeration between the measurements. The gas concentration was measured using gas chromatography. The mean microbial respiration rate (μL·g^{-1} peat dry mass) was calculated as the mean of the five individual measurements.

2.5. Greenhouse gas concentrations in the soil

Gas concentrations in the surface soil layer (at 5 and 15 cm depths) were measured using samplers, which consisted of 2-m-long silicon tubes sealed at both ends and connected to a 1-m-long plastic pipe. This technique allows for the equilibration of soil gas concentrations with the surrounding liquid phase (Kammann et al. 2001), thereby facilitating gas sampling with syringes from each tube. We used 10 mL syringes to collect the gas samples, which were then transferred into 20 mL vacuum tubes. The samples were stored in a fridge before measurement of CO_2, methane (CH_4), and nitrous oxide (N_2O) concentrations. The tubes were installed in the soil in July 2013 and were sampled the first time 2 days after installation (Kammann et al. 2001). Sampling was continued monthly over the growing season in 2014 (from May to August). Due to technical problems, N_2O was analyzed only in 2013. In total, 720 gas concentration samples were analyzed.

2.6. Greenhouse gas emissions and water table

In situ CO_2 and CH_4 emissions were measured using cylindrical aluminum chambers (diameter: 31.5 cm; height: 30.5 cm) (Alm et al. 2007), which were placed at a fixed point within the plots (total: 72 measurement points). Vegetation was not removed from the measured area; therefore, the CO_2 emissions consisted of both autotrophic and heterotrophic respiration. The air inside the chambers was mixed by a fan with dimensions 8 cm × 8 cm × 2.5 cm. The gas samples were taken with a 20 mL syringe at 5, 15, 25, and 35 min after the chamber was closed, and were afterward transferred into flushed, 20 mL vacuum tubes. The tubes were kept in a fridge before analysis with Agilent Technologies 7890A gas chromatograph and Gilson GX-271 liquid handler, similarly to Korrensalo et al. (2018). During gas sampling, we measured air temperature inside the chamber, as well as soil temperatures at the surface and at 5, 15, and 30 cm depths. The chamber measurements were performed five times over the growing season (from May to September) in 2014. In total, 1440 gas samples were analyzed to calculate soil CO_2 and CH_4 emissions (based on the linear change in gas concentration over time with respect to chamber volume and temperature).

For water table measurements we used predrilled polyvinyl chloride tubes which were placed next to the plots for greenhouse gas emissions. Water table was measured during 2014 simultaneously with samplings for greenhouse gas emissions and concentrations.

2.7. Statistical analyses

All variables subjected to statistical analysis were tested for normality of distribution with the Shapiro–Wilk test (Shapiro and Wilk 1965) and homogeneity of distribution with the Bartlett test (Bartlett and Fowler 1937). We applied a linear mixed-effects model (eq. 2) to study the impact of machine traffic and consequent soil deformation over time on living moss biomass; annual root production at a specific depth (0–10, 10–20 cm); microbial biomass carbon; CO_2 production potential; rate of cellulose decomposition at certain depth (0–5, 5–10, 10–20, and 20–30 cm). Disturbance class and age class (with an interaction term) were used as fixed effects, while sites and plots were considered as random effects. *p* values were calculated by the likelihood ratio test. The analysis was conducted in R language for statistical computing (R Core Team 2015), where the lme4 package (Bates et al. 2015) was used to perform the mixed-effects analysis and emmeans package (Lenth 2021) was used for post hoc analysis.

$$y_{ij} = \beta_0 + \beta_1 AC2_i + \beta_2 AC3_i + \beta_3 DC1_{ij} + \beta_4 DC2_{ij} + \beta_5 AC2_i DC1_{ij} + \beta_6 AC3_i DC1_{ij} + \beta_7 AC2_i DC2_{ij} + \beta_8 AC3_i DC2_{ij} + a_i + b_{ij} + \varepsilon_{ij} \quad (2)$$

where y_{ij} is the response variable in site *i* and plot *j*; $\beta_0, \ldots, \beta_8$ are parameters; AC2 and AC3 are dummy variables assigning the age class; DC1 and DC2 are dummy variables assigning the disturbance class; a_i is the random effect of site $i = (1, \ldots, 6)$; b_{ij} is the random effect of plot $j = (1, \ldots, 72)$; ε_{ij} is residual variance.

We applied multivariate methods to analyze whether and how vegetation composition and PLFA profiles were impacted by machine traffic and time since harvesting. Due to the large differences in species composition between plots in the vegetation data, we applied Detrended Correspondence Analysis (DCA) to study the variation in vegetation and its relationship to disturbance class (DC) and age class (AC). Principal Components Analysis

(PCA) was used to distinguish corresponding patterns within the PLFA data. In PCA, relationships between the multivariate PLFA data and environmental variables (DC, AC) and their interactions were quantified indirectly through regression of environmental gradients on the ordination axes that describe maximum variability. The PLFA data was standardized to reduce the impact of dominant PLFAs. The analyses were conducted with Canoco 5 (Ter Braak and Smilauer 2012).

3. Results

3.1. Vegetation

Vegetation data included 23 species, 9 of which were mosses and 14 were vascular plants (Appendix Table A1). The recently disturbed plots (DC1 and DC2 of AC1) showed a distinct plant species composition (Figs. 2*a* and 2*b*), which can be seen as their separation from the other plots along DCA Axis 1. Sedges, such as *Eriophorum vaginatum* and *Carex canescens*, and mosses, such as *Aulacomnium palustre* and *Sphagnum magellanicum*, were prevalent in the disturbed plots of AC1, while peatland and forest dwarf shrubs, such as *Vaccinium uliginosum* and *V. vitis-idaea* were typical of the other plots (left end of DCA Axis 1 in Fig. 2*a*). The species composition in the disturbed plots changed with time since harvest from AC2 to AC3, as seen in the variation along DCA Axis 2. Forest herbs, such as *Trientalis europaea* and *Dryopteris carthusiana*, and dwarf shrubs, such as *Calluna vulgaris*, were prevalent in the disturbed plots of AC2 but not in AC3.

Living moss biomass was decreased by disturbance, but only in in AC1 sites (Table 3). While control plots (AC1, DC0) had a mean living moss biomass of 608 $g{\cdot}m^{-2}$, in plots with deep ruts living moss was completely removed (AC1, DC2) and in plots with shallow ruts (AC1, DC1) moss biomass was reduced to 145 $g{\cdot}m^{-2}$. Despite such drastic decrease, the older sites did not exhibit any significant difference between disturbed and control plots, which implies that there is no lasting impact on the living moss biomass. This age class specific impact was verified by the significant interaction effect of age class and disturbance on living moss biomass (Appendix Table A2) and by the following pairwise comparison (Table 3).

In general, root biomass production was greatest in the upper 10 cm peat layer (Table 3) but was significantly decreased by disturbance, as seen in the results of the linear mixed-effects model (Appendix Table A2) and following pairwise comparisons (Table 3). Root production in the disturbed plots (DC1, DC2) of AC1 was only 21%–36% of the root production in the undisturbed plots (DC0). Recovery in root production could already be detected in AC2, where only the severely disturbed plots (DC2) showed decreased production (Table 3). In AC3, root production did not differ between the control (DC0) and the disturbed plots (DC1 and DC2). Root production in the 10–20 cm peat layer was not decreased by disturbance. However, root production was greater in the lower peat layer in the disturbed plots (DC1, DC2) of AC3 than in the other plots.

3.2. Microbiology

PCA analysis of the PLFA profiles did not reveal any clear changes in the microbial community after disturbance (Appendix Fig. A1). There was only a slight shift in the microbial community of the disturbed plots (DC1 and DC2) of AC3 along PCA Axis 2. Neither microbial biomass derived from PLFA or C_{mic} determined by FE were impacted by traffic (Appendix Tables A3 and A4). The average microbial biomass (± standard deviation) calculated with PLFA profiles for all age and disturbance classes combined was 1.8 (±0.62) $\mu mol{\cdot}g^{-1}$. Bacteria were prevalent in the total microbial biomass with the bacteria-to-fungi ratio equal to 8.2. Average C_{mic} detected with FE was 2.56 (±1.24) $mg{\cdot}g^{-1}$.

3.3. Biological activity

The CO_2 production potential had a twofold increase in recently disturbed plots (AC1, DC1, and DC2) in comparison to control plots (AC1, DC0) (Fig. 3). In AC2, the CO_2 production potential in the

Fig. 2. Detrended correspondence analysis (DCA) of plant species showing the variation in (*a*) species composition among plots belonging to various (*b*) disturbance classes within each age class. Eigenvalues for each axis are given in parentheses. Species abbreviations are presented in Appendix Table A1. Age classes: AC1, <1 year since thinning; AC2, 4–5 years since thinning; AC3, 14–15 years since thinning. Disturbance classes: DC0, undisturbed; DC1, rut depth < 0.2 m; DC2, rut depth > 0.2 m. [Colour online.]

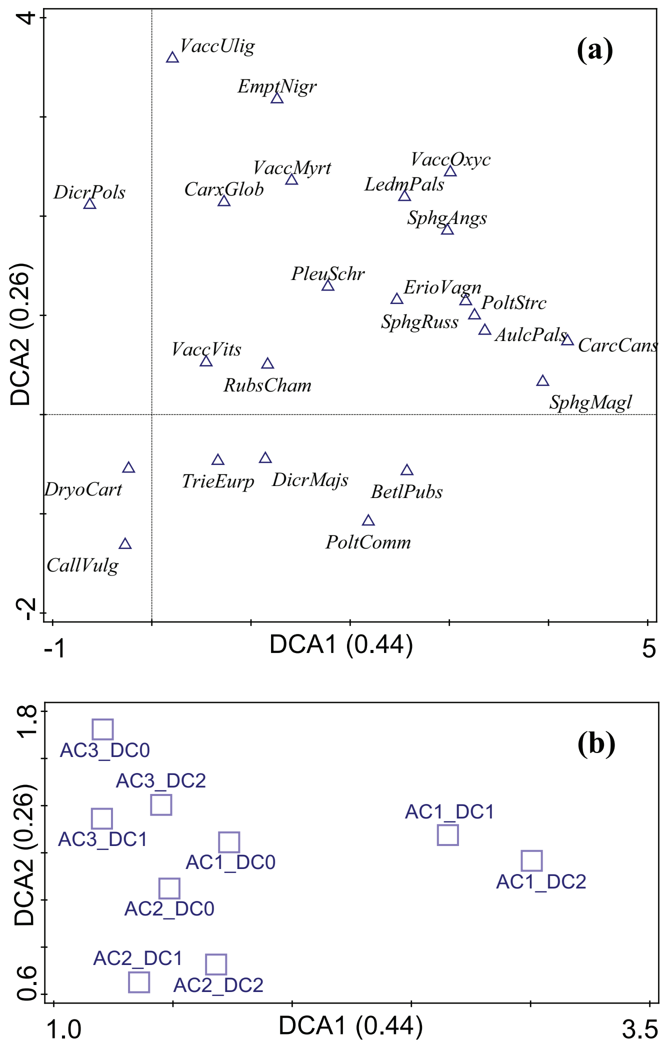

moderately disturbed plots (DC1) was similar to the potential in control plots (DC0). However, the potential was still high in the severely disturbed plots (AC2, DC2). This age class specific impact (Fig. 3; Appendix Table A5) suggests that the recovery of CO_2 production potential depends on the extent of disturbance, being more rapid after moderate disturbance.

The rate of cellulose decomposition was not influenced by the disturbance or age class (Appendix Fig. A2 and Table A5). Greatest decomposition rates, approx. 0.68$\cdot year^{-1}$ on average, occurred in the upper 5 cm layer of peat and decreased with depth to 0.2$\cdot year^{-1}$ in the two deeper layers (10–20 and 20–30 cm).

3.4. Greenhouse gas concentrations and emissions

Soil CO_2 concentrations increased in response to disturbance, as seen from the results of the mixed-effects model for CO_2 and following pairwise comparison (Table 4; Appendix Table A6). Overall, the high temporal variation in CO_2 concentrations were observed at 15 cm depth (Appendix Fig. A3). In the recently disturbed plots

Table 3. Average moss biomass and root production in two different soil layers, by age and disturbance classes.

			Root production ($g \cdot m^{-2} \cdot year^{-1}$) in:	
Age class	Disturbance class	Moss biomass ($g \cdot m^{-2}$)	0–0.1 m layer	0.1–0.2 m layer
AC1	DC0	608 (140) a	869 (283) a	218 (165) a
AC1	DC1	145 (225) bc	180 (133) b	160 (102) a
AC1	DC2	0 (0) b	316 (46) bcd	194 (95) a
AC2	DC0	477 (164) ad	686 (272) ac	270 (220) a
AC2	DC1	409 (149) acd	893 (417) a	189 (87) a
AC2	DC2	353 (216) acd	226 (92) bd	193 (142) a
AC3	DC0	391 (133) acd	934 (194) a	331 (200) a
AC3	DC1	241 (168) bcd	719 (129) ac	680 (211) b
AC3	DC2	353 (59) acd	676 (344) acd	547 (217) ab

Note: Standard deviation in parentheses. Different lowercase letters in a column indicate significant ($p < 0.05$) differences in interaction effects of age class and disturbance by Tukey pairwise comparison. Age classes: AC1, <1 year since thinning; AC2, 4–5 years since thinning; AC3, 14–15 years since thinning. Disturbance classes: DC0, undisturbed; DC1, rut depth <0.2 m; DC2, rut depth >0.2 m.

Table 4. Average soil carbon dioxide (CO_2) and methane (CH_4) concentrations, by age and disturbance classes.

		CO_2 concentration ($\mu L \cdot L^{-1}$) at:		CH_4 concentration ($\mu L \cdot L^{-1}$) at:	
Age class	Disturbance class	5 cm depth	15 cm depth	5 cm depth	15 cm depth
AC1	DC0	1 592 (1 141) a	3 199 (2 962) a	153 (483) a	657 (4 737) a
AC1	DC1	20 700 (10 665) bc	32 039 (15 813) b	1 665 (5 156) a	15 135 (21 599) ab
AC1	DC2	27 163 (17 370) b	48 811 (19 856) c	2 330 (4 986) a	19 489 (30 196) ab
AC2	DC0	1 390 (748) a	3 483 (3 942) a	1 491 (5 720) a	6 399 (27 833) a
AC2	DC1	3 400 (2 982) a	7 116 (5 248) ad	6 (14) a	9 (21) a
AC2	DC2	11 085 (13 733) ac	20 996 (22 400) bd	22 118 (46 115) b	45 482 (85 299) b
AC3	DC0	1 279 (611) a	3 741 (1 881) a	4 (6) a	2 (2) a
AC3	DC1	1 725 (908) a	6 546 (4 940) ad	4 (6) a	4 (6) a
AC3	DC2	6 853 (9 65) a	10 823 (12 721) ad	1 034 (2 594) a	4 372 (11 277) a

Note: Values are the means (standard deviations). Values followed Different lowercase letters in a column indicate significant ($p < 0.05$) differences in interaction effects of age class and disturbance by Tukey pairwise comparison. Age classes: AC1, <1 year since thinning; AC2, 4–5 years since thinning; AC3, 14–15 years since thinning. Disturbance classes: DC0, undisturbed; DC1, rut depth <0.2 m; DC2, rut depth >0.2 m. Standard deviation in parentheses.

Fig. 3. Carbon dioxide (CO_2) production potential per gram of soil dry mass. Error bars indicate ± standard deviation. DC0, DC1, and DC2 denote disturbance classes 0, 1, and 2, respectively. Different lowercase letters above the bars indicate significant ($p < 0.05$) differences in interaction effects of age class and disturbance by Tukey's pairwise comparison. Age classes: 1, <1 year since thinning; 2, 4–5 years since thinning; 3, 14–15 years since thinning. Disturbance classes: DC0, undisturbed; DC1, rut depth <0.2 m; DC2, rut depth >0.2 m.

(DC1, DC2 of AC1), CO_2 concentrations at 5 cm and 15 cm depths were clearly greater than in the control plots (Table 4). A severe disturbance effect still existed in the older age classes (AC2 and AC3), where CO_2 concentrations were greater in DC2 (Table 4). Overall, the greatest CO_2 concentrations were found in the deeper peat layer (15 cm) (Table 4; Appendix Fig. A3).

CH_4 concentrations in peat showed similar trends as CO_2 concentrations (Table 4). However, in contrast to CO_2 concentrations a significant increase in CH_4 as a response to disturbance was only observed for the deeper peat layer (15 cm) (Appendix Table A6). Higher mean concentrations were still observed in older plots of DC2. CH_4 concentrations showed high temporal variation within the measurement period and consequently were significantly influenced by the measurement date (Appendix Fig. A4). Overall, the highest CH_4 concentrations, as with CO_2, were found at the deeper peat layer (15 cm) (Table 4; Appendix Fig. A4).

Soil N_2O concentrations were measured only in October 2013 (Table 5) and similarly to CH4 were impacted only in the deeper peat layer (15 cm) (Appendix Table A7). In contrast to the carbon gases, N_2O concentrations at 15 cm depth were greatest at the control plots (0.35 $\mu L \cdot L^{-1}$; AC1, DC0) and decreased with disturbance to 0.17 $\mu L \cdot L^{-1}$ (AC1, DC1) and 0.08 $\mu L \cdot L^{-1}$ (AC1, DC2) (Table 5).

In contrast to the soil concentrations, CO_2 and CH_4 emissions were not impacted by disturbance (Table 6), although the disturbed plots DC1 and DC2 were wetter with higher water table level than the undisturbed control (DC0) in all age classes (Appendix Fig. A5). CO_2 emissions that were composed of both heterotrophic and autotrophic respiration ranged from 216 to 18 371 $mg \cdot m^{-2} \cdot day^{-1}$. For CH_4, the sites varied between sink and source to atmosphere, the fluxes ranging from −70 to 186 $mg \cdot m^{-2} \cdot day^{-1}$ (negative values indicate uptake). However, the CH_4 fluxes were mostly small (25% of values were lower than −0.51 $mg \cdot m^{-2} \cdot day^{-1}$ while 75% of values were lower than 0.96 $mg \cdot m^{-2} \cdot day^{-1}$).

Table 5. Average soil nitrous oxide (N_2O) concentrations, by age and disturbance classes.

		N_2O concentration ($\mu L \cdot L^{-1}$) at:	
Age class	Disturbance class	5 cm depth	15 cm depth
AC1	DC0	0.40 (0.03) a	0.35 (0.09) a
AC1	DC1	0.35 (0.15) a	0.17 (0.08) bc
AC1	DC2	0.73 (1.33) a	0.08 (0.04) b
AC2	DC0	0.37 (0.07) a	0.35 (0.12) ac
AC2	DC1	0.40 (0.03) a	0.39 (0.05) ac
AC2	DC2	0.27 (0.18) a	0.26 (0.17) abc
AC3	DC0	0.39 (0.01) a	0.38 (0.02) ac
AC3	DC1	0.40 (0.04) a	0.38 (0.04) ac
AC3	DC2	0.33 (0.10) a	0.32 (0.12) ac

Note: Different lowercase letters in a column indicate significant ($p < 0.05$) differences in interaction effects of age class and disturbance by Tukey pairwise comparison. Age classes: AC1, <1 year since thinning; AC2, 4–5 years since thinning; AC3, 14–15 years since thinning. Disturbance classes: DC0, undisturbed; DC1, rut depth <0.2 m; DC2, rut depth >0.2 m. Standard deviation in parentheses.

Table 6. Average carbon dioxide (CO_2) and methane (CH_4) emissions, by age and disturbance classes.

Age class	Disturbance class	CO_2 emissions ($mg \cdot m^{-2} \cdot day^{-1}$)	CH_4 emissions ($mg \cdot m^{-2} \cdot day^{-1}$)
AC1	DC0	2249 (3295)	−0.50 (6.87)
AC1	DC1	1879 (2504)	15.76 (87.78)
AC1	DC2	2639 (3113)	10.58 (99.92)
AC2	DC0	1891 (3082)	143.10 (1091.56)
AC2	DC1	1537 (3362)	−1.50 (9.07)
AC2	DC2	1782 (2303)	0.37 (9.20)
AC3	DC0	1927 (4735)	−1.11 (7.54)
AC3	DC1	3272 (4614)	1.91 (6.80)
AC3	DC2	1090 (2797)	0.19 (2.17)

Note: Age classes: AC1, <1 year since thinning; AC2, 4–5 years since thinning; AC3, 14–15 years since thinning. Disturbance classes: DC0, undisturbed; DC1, rut depth <0.2 m; DC2, rut depth >0.2 m. Standard deviation in parentheses.

4. Discussion

We investigated the response of vegetation and soil biological properties to the soil disturbance induced by forest machinery in drained peatland forests using a chronosequence that covered a 15-year period following harvesting. Our data showed concurrent and significant changes in vegetation composition, root production, moss biomass, CO_2 production, and soil gas concentrations (CO_2, CH_4, N_2O). The strongest effects of disturbance were observed in the recently disturbed plots (DC1 and DC2, AC1). From then on, all the biological properties examined gradually recovered and began to resemble the properties of the control plots (DC0) in the older age classes (AC2 and AC3). Such recovery has been previously found to take place with the soil physical properties (Lepilin et al. 2019). The recovery rates here varied from rapid (defined here as the recovery observed in AC2) to slow (recovery observed in AC3).

The change in vegetation structure following mechanical disturbance was demonstrated by the differences in plant community composition between disturbed (DC1 and DC2) and undisturbed (DC0) plots in the AC1 sites. The cover of sedges (e.g., *Eriophorum vaginatum* and *Carex canescens*) that typically benefit from disturbance events, such as clearcutting and restoration (Komulainen et al. 1999), was significantly greater in the recently disturbed plots (DC1 and DC2, AC1). That is in agreement with Davidson et al. (2021) who reported a shift in vegetation community of seismic lines (linear disturbances in peatlands) to sedge dominance. The shifts in vegetation composition are likely caused by the greater nutrient availability after harvesting following mechanical crushing of fresh organic matter and peat aggregates during deformation. Decreased competition with the tree stand after tree biomass removal might also benefit ground-layer plant species. However, the later recovery observed for forest herbs and dwarf shrubs is more likely to be driven by the closure of the canopy, which had a negative effect on several wetland species.

Living moss biomass was severely disturbed. The immediate decrease in moss biomass in the recently disturbed plots (DC1 and DC2, AC1) was directly caused by mechanical removal of the moss by wheels/tracks during harvesting. However, there was a rapid recovery in moss biomass, and in the cover of *Sphagnum* mosses, such as *Sphagnum angustifolium* and *S. magellanicum*, which increased rapidly after the initial decrease. Our findings agree with rapid responses previously found for mosses, both in the sensitivity to disturbance and in the recovery. In general, it has been reported that disturbance has a negative effect on moss cover (Deans et al. 2003). For instance, in agreement with this and our findings, Hannerz and Hånell (1997) found that moss cover was significantly reduced after clearcutting. In agreement with rapid recovery for *Sphagnum* and slower for *Pleurozium schreberii* found in our study, Zhu et al. (2019) reported that *Sphagnum* mosses with greater photosynthetic adaptation have a high proliferation potential after clearcutting and the subsequent increase in light availability, while feathermosses tend to decrease. Similarly, Deane et al. (2020) found *Sphagnum* moss domination on seismic lines in Canada.

The observed decrease in root production in the upper peat layer (10 cm) of the recently disturbed plots (DC1 and DC2, AC1) is most likely connected with tree biomass removal and consequent decrease of fine root production. In addition, the decreased soil aeration observed in the recently formed ruts in our study sites and the reduced macropore size (Lepilin et al. 2019) can result in a shift to anaerobic processes (Frey et al. 2009) and create a hostile environment that impedes the growth of fine roots. Similarly, root necrosis can be found in mineral soils with a high clay content that causes impermeable layers (Rhoades et al. 2003), which are suboptimal conditions for root growth. The recovery of root production in our study sites, especially in the deeper peat layer, may be related to the increase of sedges that are able to tolerate anoxic soil conditions.

The CO_2 concentrations (2%–6%) observed in the ruts of the recently disturbed plots (depth: 15 cm; DC1 and DC2, AC1) and in the undisturbed plots (DC0, AC1) (0.3%–0.8%) are similar to that of other studies under forest vegetation (Neruda et al. 2010; Magagnotti et al. 2012; Allman et al. 2016; Jankovský et al. 2019). Neruda et al. (2010) reported that a concentration of 0.6% CO_2 in soil air is a boundary value that is indicative of significant changes in the soil structure with consequences for the growth of roots. Erler and Güldner (2002) stated that a CO_2 concentration >2% may entirely impede the potential for biological recovery: in all recently disturbed plots (DC1 and DC2, AC1), the CO_2 concentration in the soil exceeded that value several-fold. Aside from the elevated CO_2 concentrations in the ruts, we also found greater spatial variability in the severely disturbed plots (DC2) (Appendix Fig. A3), most likely related to the structural changes in the soil induced by machine traffic. CO_2 concentrations in the severely disturbed plots also showed strong spatial variability with regard to time since harvesting; the lower CO_2 levels that were generally measured in the older sites suggest that the soil has recovered over the course of 15 years.

As with CO_2 concentrations, disturbance appeared to increase the CO_2 production potential of the peat soil. In general, CO_2 production is driven by both decomposition of organic matter and root respiration (Ball et al. 1999). However, as the CO_2 potential was measured in the laboratory from peat without roots and root production was decreased by disturbance, this allows us to conclude that the increase in the CO_2 production potential was directly driven by an increased rate of decomposition. Most likely, this increase was due to rutting, which brought fresh peat from the layer below to the surface, and the mechanical milling by forest machinery that provided crushed organic matter particles to decomposers.

Surprisingly, the increased CO_2 production potential and soil CO_2 concentrations were not reflected in net soil CO_2 emissions or in the rate of cellulose decomposition, which did not differ between the ruts and the adjacent non-impacted control areas. This lack of response was however in line with the lack of clear difference in microbial biomass and community structure. Contradictory responses of soil CO_2 emissions to disturbance were also previously observed in other studies. For instance, while Novara et al. (2012) reported elevated CO_2 emissions after moderate compaction due to enhanced microbial mineralization of freshly exposed organic matter, Pearson et al. (2012) observed no effect from either mounding or scalping in a clear-cut area. While it is difficult to explain why CO_2 and CH_4 concentrations in the soil increased and the emissions were unimpacted (both measured in the field), our finding is in line with a previous study that reported an uncoupling between CO_2 emissions and production in the soil layers (Barry et al. 2020).

In contrast to CO_2, CH_4 concentrations were significantly greater only at 15 cm depth in the recently disturbed plots (DC1 and DC2, AC1). The rut formation, which had altered the site microtopography, produced water-induced anaerobic conditions with higher water table. The rather rapid recovery could potentially be linked to a shortage of easily available substrates for methanogenesis after the substrates produced from mechanical milling had been rapidly consumed. This suggestion about the mechanism agrees with higher water table found in disturbed plots also from older age classes. Earlier, harvesting has been found to alter soil bulk density and increase water retention due to the reduction of mesopore volume (Lepilin et al. 2019), which hinders soil aeration. This is common on mineral soils after machinery impact (Frey et al. 2009; Magagnotti et al. 2012; Cambi et al. 2015; Grigorev et al. 2021) and leads to increased anaerobic conditions. Yet again, we observed no difference in the net emissions of CH_4 between the ruts and the adjacent non-impacted control areas. In contrast to our study, Strack et al. (2018) found that increased bulk density values associated with track formation and increased graminoid cover led to increased CH_4 emissions from Canadian peatland sites. The lack of an observed response (or better, the surprising lack of patterns) in our study is interesting as we observed both increased bulk density and increase in sedge cover, as well as increased water table level and soil CH_4 concentration. This points out that CH_4 emissions in our sites were controlled by high oxidation rather than low production, and therefore, the logging trails in drained peatland forests may represent high CH4 emission potential directly after the disturbance. Overall, the values of the studied parameters are in line with earlier studies; e.g., the measured rate of cellulose decomposition and the pattern with depth are in agreement with an earlier study in drained and undrained peatlands (Ojanen et al. 2017), and the measured CH_4 and CO_2 emissions are typical of drained peatland forests (Ojanen et al. 2010). This would suggest that the more surprising patterns that we found here are not due to inaccuracies in our measurements.

Our results indicate a high level of resilience of the peat soil and relatively rapid recovery following the disturbance caused by thinning operations. Also, our findings suggest that the peat soil may recover from the relatively frequent harvest cycles that would follow a shift to continuous-cover forestry, which has been suggested to mitigate some of the harmful environmental impacts of traditional, rotation-based forestry on peatlands (Nieminen et al. 2018). This is in contrast to mineral soils where slow recovery rates (Magagnotti et al. 2012) set a limit on the more frequent loggings associated with continuous-cover forestry. A 15-year harvest interval has been suggested to produce the most optimal economic returns in spruce-dominated peatland stands under continuous-cover forestry (Juutinen et al. 2021). How continuous-cover forestry is realized in practice is still not clear, however, and the recovery of the soil following repeated harvest cycles may still warrant further study. It is also important to note that clearcutting usually causes greater levels of soil disturbance in comparison to thinnings, which will probably lead to a longer recovery period.

Conclusions

We studied the impact of forest machinery traffic on the soil biology of drained peatlands during forest thinning operations. The chronosequence study indicated a high level of resilience in the structure and functioning of drained peatlands to thinning: After a short-term disturbance, the ecosystem was able return to its original state within the time scale (15 years) covered in the sampling. The study adds a biological assessment of peat soils to the previously reported change in physical properties (Lepilin et al. 2019) at different levels of soil disturbance. These results are important for the evaluation of (*a*) the negative effects that forest machinery imposes on peatland forests, (*b*) soil sustainability, and (*c*) the threshold of soil disturbance where restorative measures must be conducted to mitigate physically and biologically damaged soils. Our results show that thinning does not cause irreversible changes to peat soil properties and indicate that forestry practices which include mechanical harvesting are sustainable in peatlands in the perspective of soil biogeochemistry, as the peat appears to be resilient to disturbance. However, it is important to note that the study considered only first-time thinning operations and more frequent or severe disturbances might have higher potential for long lasting impact to soil's properties.

Funding

Financial support from University of Eastern Finland (Faculty of Science and Forestry, Cross-Border University (CBU) Program, and Doctoral Programme in Forests and Bioresources (FORES) made the study possible. The Academy of Finland project 138041 and The Atmosphere and Climate Competence Center (ACCC) Flagship (337550) contributed to the study.

Acknowledgements

We are deeply grateful to Aino Korrensalo, Vladimir Yazov, María Luisa Gutiérrez, Janne Sormunen, Laura Kettunen, Maini Mononen, and Leena Kuusisto for all their help with laboratory and field work.

References

Allman, M., Jankovský, M., Messingerová, V., and Allmanová, Z. 2016. Changes of carbon dioxide concentration in soils caused by forestry machine traffic. Central Eur. For. J. **62**(1): 23–28. doi:10.1515/forj-2016-0003.

Alm, J., Shurpali, N.J., Tuittila, E.-S., Laurila, T., Maljanen, M., Saarnio, S., and Minkkinen, K. 2007. Methods for determining emission factors for the use of peat and peatlands flux measurements and modelling. Boreal Environ. Res. **12**(2): 85–100.

Ball, B.C., Scott, A., and Parker, J.P. 1999. Field N2O, CO2 and CH4 fluxes in relation to tillage, compaction and soil quality in Scotland. Soil Tillage Res. **53**(1): 29–39. doi:10.1016/S0167-1987(99)00074-4.

Barry, S., Gilmer, A., Cassidy, J., McGovern, E., and Byers, V. 2020. A primer on gas phase CO2 production and transport in peatland soils. Land Sci. **2**(2): 45. doi:10.30560/ls.v2n2p45.

Bartlett, M.S., and Fowler, R.H. 1937. Properties of sufficiency and statistical tests. Proc. R. Soc. Ser. A Math. Phys. Sci. **160**(901): 268–282. doi:10.1098/rspa.1937.0109.

Bates, D., Mächler, M., Bolker, B., and Walker, S. 2015. Fitting linear mixed-effects models using lme4. J. Stat. Softw. **67**(1): 1–48. doi:10.18637/jss.v067.i01.

Bettinger, P., Armlovich, D., and Kellogg, L.D. 1994. Evaluating area in logging trails with a geographic information system. Trans. ASAE, **37**(4): 1327–1330. doi:10.13031/2013.28214.

Bodelier, P., Libochant, J.A., Blom, C., and Laanbroek, H.J. 1996. Dynamics of nitrification and denitrification in root-oxygenated sediments and adaptation of ammonia-oxidizing bacteria to low-oxygen or anoxic habitats. Appl. Environ. Microbiol. **62**(11): 4100–4107. doi:10.1128/aem.62.11.4100-4107.1996. PMID:16535441.

Cambi, M., Certini, G., Neri, F., and Marchi, E. 2015. The impact of heavy traffic on forest soils: A review. For. Ecol. Manag. **338**: 124–138. doi:10.1016/j.foreco.2014.11.022.
Chow, T.L., Rees, H.W., Ghanem, I., and Cormier, R. 1992. Compactibility of cultivated sphagnum peat material and its influence on hydrologic characteristics. Soil Sci. **153**(4): 300–306. doi:10.1097/00010694-199204000-00006.
Cudzik, A., Brennensthul, M., Białczyk, W., and Czarnecki, J. 2017. Damage to soil and residual trees caused by different logging systems applied to late thinning. Croatian J. For. Eng. **38**(1): 83–95.
Davidson, S.J., Goud, E.M., Franklin, C., Nielsen, S.E., and Strack, M. 2020. Seismic line disturbance alters soil physical and chemical properties across boreal forest and peatland soils. Front. Earth Sci. **8**: 281. doi:10.3389/feart.2020.00281.
Davidson, S.J., Goud, E.M., Malhotra, A., Estey, C.O., Korsah, P., and Strack, M. 2021. Linear disturbances shift boreal peatland plant communities toward earlier peak greenness. J. Geophys. Res.: Biogeosci. **126**(8): e2021JG006403. doi:10.1029/2021JG006403.
Deane, P.J., Wilkinson, S.L., Moore, P.A., and Waddington, J.M. 2020. Seismic lines in treed boreal peatlands as analogs for wildfire fuel modification treatments. Fire, **3**(2): 21. doi:10.3390/fire3020021.
Deans, A.M., Malcolm, J.R., Smith, S.M., and Carleton, T.J. 2003. A comparison of forest structure among old-growth, variable retention harvested, and clearcut peatland black spruce (*Picea mariana*) forests in boreal northeastern Ontario. For. Chron. **79**(3): 579–589. doi:10.5558/tfc79579-3.
Echiverri, L.F.I., Macdonald, S.E., and Nielsen, S.E. 2020. Disturbing to restore? Effects of mounding on understory communities on seismic lines in treed peatlands. Can. J. For. Res. **50**(12): 1340–1351. doi:10.1139/cjfr-2020-0092.
Eliasson, L. 2005. Effects of Forwarder Tyre Pressure on Rut Formation and Soil Compaction. Silva Fenn. Monogr. **39**(4): 549–557. doi:10.14214/sf.366.
Erler, J., and Güldner, O. 2002. Technologisch differenzierte Standorte – der Weg zu einem Vertragsbodenschutz? Allgemeine Forstzeitung, (10): 484–488.
Frey, B., Kremer, J., Rüdt, A., Sciacca, S., Matthies, D., and Lüscher, P. 2009. Compaction of forest soils with heavy logging machinery affects soil bacterial community structure. Eur. J. Soil Biol. **45**: 312–320. doi:10.1016/j.ejsobi.2009.05.006.
Gaertig, T., Schack-Kirchner, H., Hildebrand, E.E., and Wilpert, K. V. 2002. The impact of soil aeration on oak decline in southwestern Germany. For. Ecol. Manag. **159**(1): 15–25. doi:10.1016/S0378-1127(01)00706-X.
Goutal, N., Parent, F., Bonnaud, P., Demaison, J., Nourrisson, G., Epron, D., and Ranger, J. 2012. Soil CO2 concentration and efflux as affected by heavy traffic in forest in northeast France. Eur. J. Soil Sci. **63**(2): 261–271. doi:10.1111/j.1365-2389.2011.01423.x.
Grigorev, I., Kunickaya, O., Burgonutdinov, A., Tikhonov, E., Makuev, V., Egipko, S., et al. 2021. Modeling the effect of wheeled tractors and skidded timber bunches on forest soil compaction. J. Appl. Eng. Sci. **19**(2): 439–447. doi:10.5937/jaes0-28528.
Groot, A. 1987. Silvicultural consequences of forest harvesting on peatlands: site damage and slash conditions. Minister of Supply and Services Canada.
Hannerz, M., and Hånell, B. 1997. Effects on the flora in Norway spruce forests following clearcutting and shelterwood cutting. For. Ecol. Manag. **90**(1): 29–49. doi:10.1016/S0378-1127(96)03858-3.
Jankovský, M., Allman, M., Allmanová, Z., Ferenčík, M., and Vlčková, M. 2019. Changes of key soil parameters five years after forest harvesting suggest slow regeneration of disturbed soil. J. Sustainable For. **38**(4): 369–380. doi:10.1080/10549811.2018.1549500.
Jordan, D., Ponder, F., and Hubbard, V.C. 2003. Effects of soil compaction, forest leaf litter and nitrogen fertilizer on two oak species and microbial activity. Appl. Soil Ecol. **23**(1): 33–41. doi:10.1016/S0929-1393(03)00003-9.
Juutinen, A., Shanin, V., Ahtikoski, A., Rämö, J., Mäkipää, R., Laiho, R., et al. 2021. Profitability of continuous-cover forestry in Norway spruce dominated peatland forest and the role of water table. Can. J. For. Res. **51**(6): 1–12. doi:10.1139/cjfr-2020-0305.
Kammann, C., Grünhage, L., and Jäger, H.-J. 2001. A new sampling technique to monitor concentrations of CH_4, N_2 O and CO_2 in air at well-defined depths in soils with varied water potential. Eur. J. Soil Sci. **52**(2): 297–303. doi:10.1046/j.1365-2389.2001.00380.x.
Kokkonen, N.A.K., Laine, A.M., Laine, J., Vasander, H., Kurki, K., Gong, J., and Tuittila, E.-S. 2019. Responses of peatland vegetation to 15-year water level drawdown as mediated by fertility level. J. Veg. Sci. **30**(6): 1206–1216. doi:10.1111/jvs.12794.
Komulainen, V.-M., Tuittila, E.-S., Vasander, H., and Laine, J. 1999. Short term effect of restoration on vegetation succession and CO2-exhange from peatland drained for forestry. J. Appl. Ecol. **36**: 636–648.
Korrensalo, A., Männistö, E., Alekseychik, P., Mammarella, I., Rinne, J., Vesala, T., and Tuittila, E.-S. 2018. Small spatial variability in methane emission measured from a wet patterned boreal bog. Biogeosciences, **15**(6): 1749–1761. doi:10.5194/bg-15-1749-2018.
Lähde, E. 1974. Rate of decomposition of cellulose in forest soils in various parts of the Nordic countries. Ann. Univ. Turku, A2, **55**: 72–78.
Laiho, R., Bhuiyan, R., Straková, P., Mäkiranta, P., Badorek, T., and Penttilä, T. 2014. Modified ingrowth core method plus infrared calibration models for estimating fine root production in peatlands. Plant Soil, **385**(1–2): 311–327. doi:10.1007/s11104-014-2225-3.
Laine, J., and Vasander, H. 2008. Suotyypit ja niiden tunnistaminen. Metsäkustannus, Helsinki.
Lenth, R.V. 2021. emmeans: Estimated Marginal Means, aka Least-Squares Means. Available from https://CRAN.R-project.org/package=emmeans.
Lepilin, D., Laurén, A., Uusitalo, J., and Tuittila, E.-S. 2019. Soil deformation and its recovery in logging trails of drained boreal peatlands. Can. J. For. Res. **49**(7): 743–751. doi:10.1139/cjfr-2018-0385.
Li, Q., Lee Allen, H., and Wollum, A.G. 2004. Microbial biomass and bacterial functional diversity in forest soils: effects of organic matter removal, compaction, and vegetation control. Soil Biol. Biochem. **36**(4): 571–579. doi:10.1016/j.soilbio.2003.12.001.
Magagnotti, N., Spinelli, R., Güldner, O., and Erler, J. 2012. Site impact after motor-manual and mechanised thinning in Mediterranean pine plantations. Biosyst. Eng. **113**(2): 140–147. doi:10.1016/j.biosystemseng.2012.07.001.
Marshall, V.G. 2000. Impacts of forest harvesting on biological processes in northern forest soils. For. Ecol. Manag. **133**(1–2): 43–60. doi:10.1016/S0378-1127(99)00297-2.
Neruda, J., Kadlec, J., Ulrich, R., and Cudzik, A. 2010. Soil carbon dioxide concentration and efflux changes in ruts after heavy machine passes. *In* FORMEC: Proceedings of Forest Engineering: Meeting the Needs of the Society and the Environment, July 11–14, 2010, Padova, Italy. pp. 11–14.
Nieminen, M., Hökkä, H., Laiho, R., Juutinen, A., Ahtikoski, A., Pearson, M., et al. 2018. Could continuous cover forestry be an economically and environmentally feasible management option on drained boreal peatlands? For. Ecol. Manag. **424**: 78–84. doi:10.1016/j.foreco.2018.04.046.
Novara, A., Armstrong, A., Gristina, L., Semple, K.T., and Quinton, J.N. 2012. Effects of soil compaction, rain exposure and their interaction on soil carbon dioxide emission. Earth Surf. Process. Landforms, **37**(9): 994–999. doi:10.1002/esp.3224.
Nugent, C., Kanali, C., Owende, P.M.O., Nieuwenhuis, M., and Ward, S. 2003. Characteristic site disturbance due to harvesting and extraction machinery traffic on sensitive forest sites with peat soils. For. Ecol. Manag. **180**(1–3): 85–98. doi:10.1016/S0378-1127(02)00628-X.
Ojanen, P., Minkkinen, K., Alm, J., and Penttilä, T. 2010. Soil-atmosphere CO2, CH4 and N2O fluxes in boreal forestry-drained peatlands. For. Ecol. Manag. **260**(3): 411–421. doi:10.1016/j.foreco.2010.04.036.
Ojanen, P., Mäkiranta, P., Penttilä, T., and Minkkinen, K. 2017. Do logging residue piles trigger extra decomposition of soil organic matter? For. Ecol. Manag. **405**: 367–380. doi:10.1016/j.foreco.2017.09.055.
Päivänen, J. 2008. Peatland forestry — the Finnish case. *In* After wise use — the future of peatlands. pp. 499–501.
Pearson, M., Saarinen, M., Minkkinen, K., Silvan, N., and Laine, J. 2012. Short-term impacts of soil preparation on greenhouse gas fluxes: a case study in nutrient-poor, clearcut peatland forest. For. Ecol. Manag. **283**: 10–26. doi:10.1016/j.foreco.2012.07.011.
Peltoniemi, K., Laiho, R., Juottonen, H., Kiikkilä, O., Mäkiranta, P., Minkkinen, K., et al. 2015. Microbial ecology in a future climate: effects of temperature and moisture on microbial communities of two boreal fens. FEMS Microbiol. Ecol. **91**: fiv062. doi:10.1093/femsec/fiv062. PMID:26066028.
Pennanen, T., Liski, J., Bååth, E., Kitunen, V., Uotila, J., Westman, C.J., and Fritze, H. 1999. Structure of the microbial communities in coniferous forest soils in relation to site fertility and stand development stage. Microb. Ecol. **38**(2): 168–179. doi:10.1007/s002489900161. PMID:10441709.
R Core Team. 2015. R: a language and environment for statistical computing. R Foundation for Statistical Computing, Vienna, Austria. Available from http://www.r-project.org.
Rhoades, C.C., Brosi, S.L., Dattilo, A.J., and Vincelli, P. 2003. Effect of soil compaction and moisture on incidence of phytophthora root rot on American chestnut (*Castanea dentata*) seedlings. For. Ecol. Manag. **184**(1): 47–54. doi:10.1016/S0378-1127(03)00147-6.
Shapiro, S.S., and Wilk, M.B. 1965. An analysis of variance test for normality (complete samples). Biometrika, **52**(3–4): 591–611. doi:10.1093/biomet/52.3-4.591.
Startsev, A.D., and McNabb, D.H. 2001. Skidder traffic effects on water retention, pore-size distribution, and van Genuchten parameters of boreal forest soils. Soil Sci. Soc. Am. J. **65**(1): 224–231. doi:10.2136/sssaj2001.651224x.
Strack, M., Softa, D., Bird, M., and Xu, B. 2018. Impact of winter roads on boreal peatland carbon exchange. Global Change Biol. **24**(1): e201–e212. doi:10.1111/gcb.13844.
Talbot, B., Rahlf, J., and Astrup, R. 2018. An operational UAV-based approach for stand-level assessment of soil disturbance after forest harvesting. Scand. J. For. Res. **33**(4): 387–396. doi:10.1080/02827581.2017.1418421.
Tan, X., Chang, S.X., and Kabzems, R. 2005. Effects of soil compaction and forest floor removal on soil microbial properties and N transformations in a boreal forest long-term soil productivity study. For. Ecol. Manag. **217**(2): 158–170. doi:10.1016/j.foreco.2005.05.061.
Ter Braak, C.J.F., and Smilauer, P. 2012. Canoco 5, Windows release (5.00).
The Plant List. 2013. The plant list. A working list of all plant species. Available from http://www.theplantlist.org/.
Uusitalo, J., and Ala-Ilomäki, J. 2013. The significance of above-ground biomass, moisture content and mechanical properties of peat layer on the bearing capacity of ditched pine bogs. Silva Fenn. **47**(3): 993. doi:10.14214/sf.993.
Vance, E.D., Brookes, P.C., and Jenkinson, D.S. 1987. An extraction method for measuring soil microbial biomass C. Soil Biol. Biochem. **19**(6): 703–707. doi:10.1016/0038-0717(87)90052-6.

Vanhatalo, K., Väisänen, P., Joensuu, S., Sved, J., Koistinen, A., and Äijälä, O. 2015. Metsänhoidon suositukset suometsien hoitoon, työopas. Tapion julkaisuja.

Voroney, R.P., Brookes, P.C., and Beyaert, R.P. 2008. Soil microbial biomass C, N, P, and S. *In* Soil sampling and methods of analysis. 2nd ed. *Edited by* M.R. Carter and E.G. Gregorich. CRC Press, Taylor & Francis, Boca Raton, Fla., USA pp. 637–652. doi:10.1201/9781420005271.

Wieder, R.K., Vitt, D.H., and Benscoter, B.W. 2006. Peatlands and the boreal forest. *In* Boreal peatland ecosystems. Springer, Berlin Heidelberg New York. pp. 1–8.

Zhu, X., Nimmo, V., Wu, J., and Thomas, R. 2019. Sphagnum outcompetes feathermosses in their photosynthetic adaptation to postharvest black spruce forests. Botany, **97**(11): 585–597. doi:10.1139/cjb-2019-0076.

Appendix A

Fig. A1. Principal components analysis (PCA) biplots of phospholipid fatty acid (PLFA)-indicated microbial community structure showing the variation in (*a*) species composition (only 10 % of PLFA profiles affected by disturbance class and age class are shown in the figure), and (*b*) among plots belonging to various disturbance classes within each age class. Eigenvalues for each axis are given in parentheses. Age classes: AC1, <1 year since thinning; AC2, 4–5 years since thinning; AC3, 14–15 years since thinning. Disturbance classes: DC0, undisturbed; DC1, rut depth <0.2 m; DC2, rut depth >0.2 m. [Colour online.]

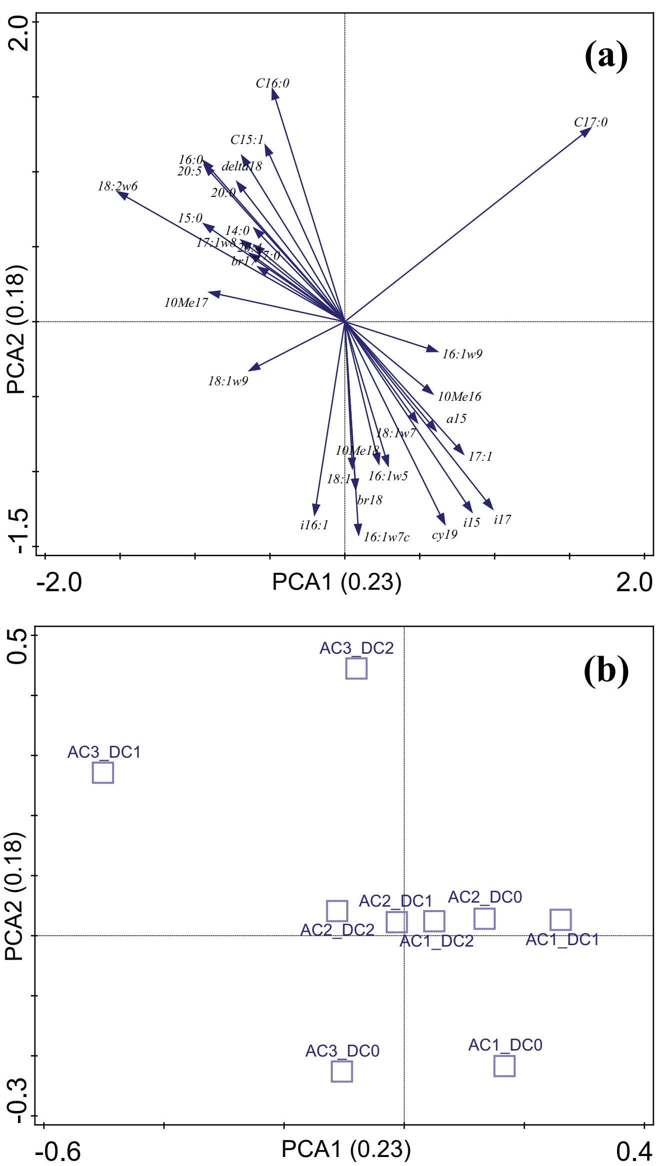

Fig. A2. Percentage of cellulose remaining after 1 year in the soil at the following depths: 0–5, 5–10, 10–20, and 20–30 cm. Error bars indicate ± standard deviation. Different lowercase letters in a column indicate significant ($p < 0.05$) differences in interaction effects of age class and disturbance by Tukey's pairwise comparison. Age classes: AC1, <1 year since thinning; AC2, 4–5 years since thinning; AC3, 14–15 years since thinning. Disturbance classes: DC0, undisturbed; DC1, rut depth <0.2 m; DC2, rut depth >0.2 m. No significant difference was found.

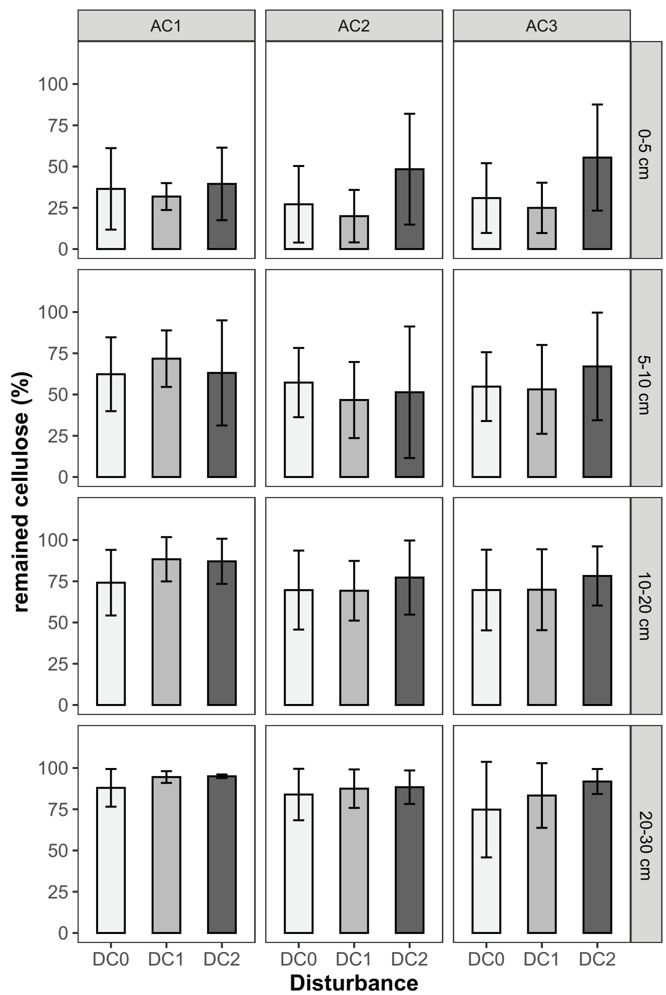

Fig. A3. Concentration of carbon dioxide (CO_2) in the soil at 15 cm depth. Panel headings are sampling times (month, year). Age classes: AC1, <1 year since thinning; AC2, 4–5 years since thinning; AC3, 15 years since thinning. Disturbance classes: DC0, undisturbed; DC1, rut depth <0.2 m; DC2, rut depth >0.2 m. Number of observations for each month: DC0 (n = 12), DC1 (n = 6), and DC2 (n = 6).

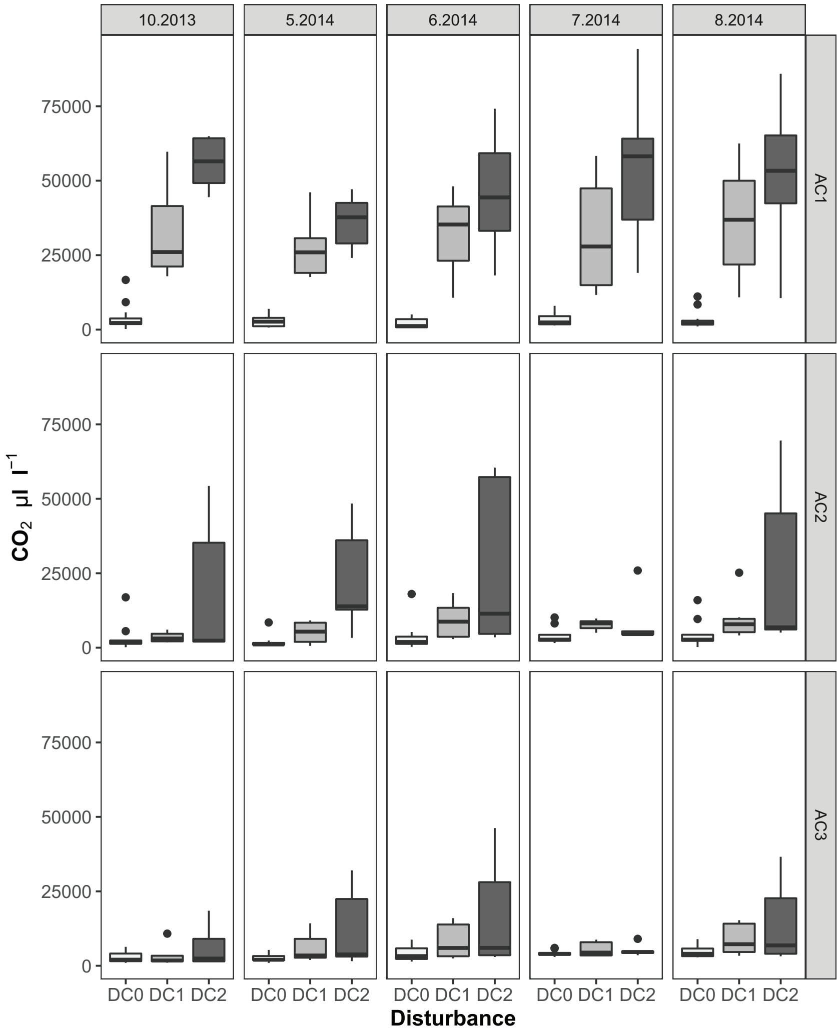

Fig. A4. Concentration of methane (CH_4) in the soil at 15 cm depth. Panel headings are sampling times (month, year). Age classes: AC1, <1 year since thinning; AC2, 4–5 years since thinning; AC3, 14–15 years since thinning. Disturbance classes: DC0, undisturbed; DC1, rut depth <0.2 m; DC2, rut depth >0.2 m. Number of observations for each month: DC0 (n = 12), DC1 (n = 6), and DC2 (n = 6).

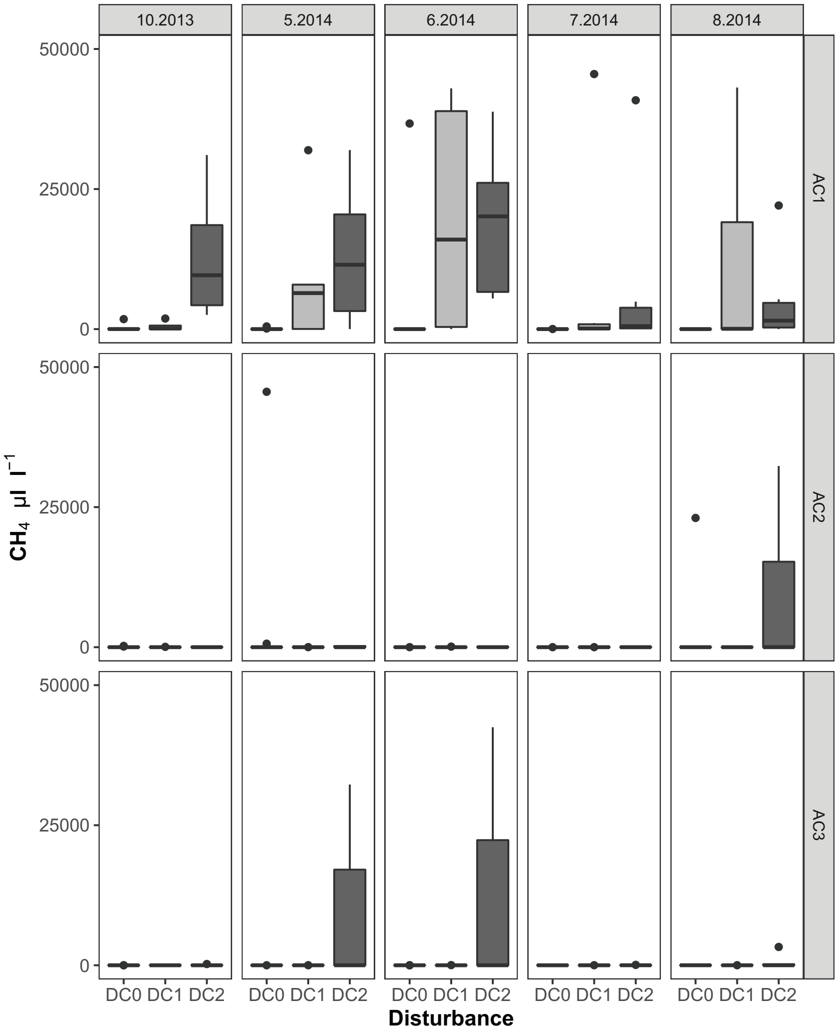

Fig. A5. Water table measured over growing season in 2014. Age classes: AC1, <1 year since thinning; AC2, 4–5 years since thinning; AC3, 14–15 years since thinning. Disturbance classes: DC0, undisturbed; DC1, rut depth <0.2 m; DC2, rut depth >0.2 m.

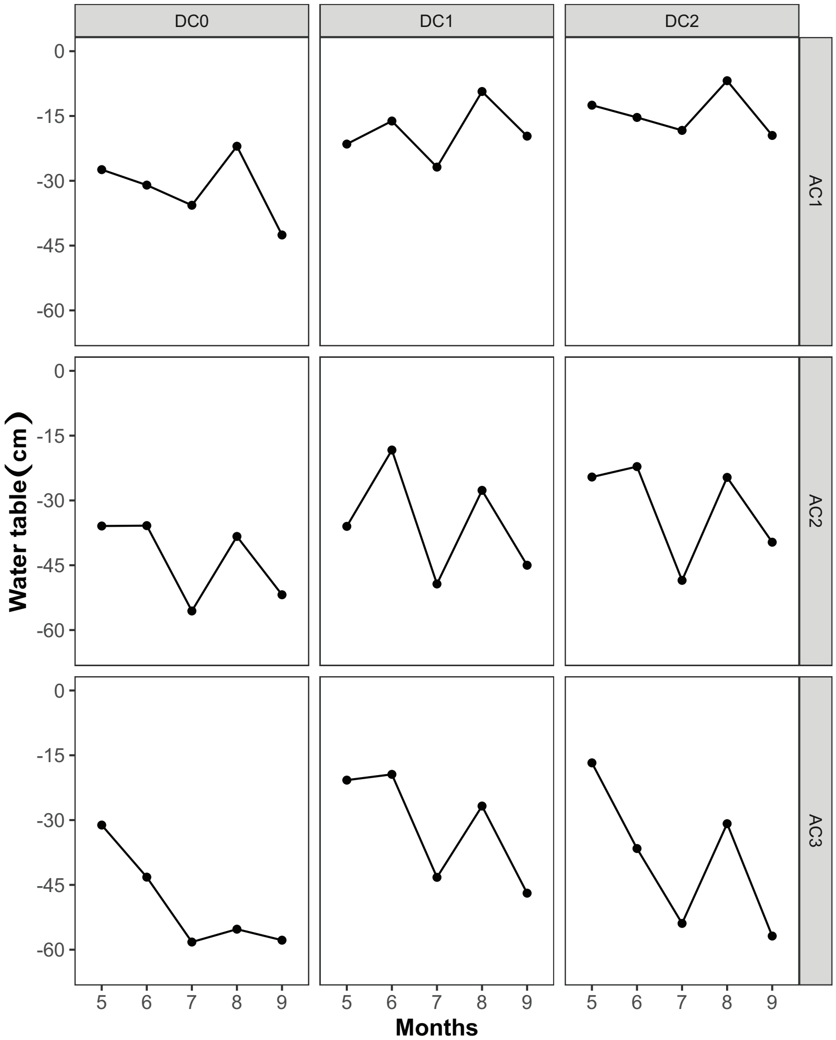

Table A1. Estimated cover (%) (mean ± standard deviation) of vascular plant species and non-vascular plant species, by disturbance and age classes.

		Estimated cover (%)								
Species	Abbreviation	AC1, DC0	AC1, DC1	AC1, DC2	AC2, DC0	AC2, DC1	AC2, DC2	AC3, DC0	AC3, DC1	AC3, DC2
Vascular plant species										
Andromeda polifolia									1	
Betula nana									4	
Betula pubescens	*BetlPubs*		2±1			4±0				
Calluna vulgaris	*CallVulg*					10	6		8	2
Carec canescens	*CarcCans*		19±21	13±17		11	5			
Carex globularis	*CarxGlob*	1			3±1	7±7	12	9±2	6±1	4
Deschampsia flexuosa							5			
Dryopteris carthusiana	*DryoCart*				10	19±16	14±9	15	12	2
Empetrum nigrum	*EmptNigr*	2±1			3±0			5±3	2±1	
Epilobium angustifolium						2±0				
Eriophorum vaginatum	*ErioVagn*	5±7	9	8	9±8	3	8±7	6±3	5	8±3
Ledum palustre	*LedmPals*	5±2	1							18
Lycopodium annotium					10			50		
Pinus sylvestris										5
Rubus chamaemorus	*RubsCham*	6±4	1		3±1	9±5	11±13	6±3	10±11	8±4
Trientalis europaea	*TrieEurp*				17±19			2±1		2
Vaccinium myrtillus	*VaccMyrt*	13±4	7	0	8±5	6	10	12±9	5±5	6±4
Vaccinium oxycoccos	*VaccOxyc*	9	5					3		1
Vaccinium uliginosum	*VaccUlig*	4±2	1		12±0	6		7±4	4	2
Vaccinium vitis-idaea	*VaccVits*	11±6	1		16±11	9±11	9±1	11±6	8±5	14±1
Non-vascular plant species										
Atrichum tenellum			6	10						
Atrichum undulatum			30	1						
Aulacomnium palustre	*AulcPals*	1	5±5	8±8	2		5±1	5	7	0
Cetraria islandica		6								
Cladonia arbuscula		11								5
Dicranum majus	*DicrMajs*	15±16			8±10	5±2	16±16			5
Dicranum polysetum	*DicrPols*		12			4	10	10±15	13±19	15±14
Dicranum scoparium			3	3						
Pleurozium schreberii	*PleuSchr*	36±21	10±13	13±5	44±23	14±16	24±15	39±33	24±22	18±19
Polytrichum commune	*PoltComm*	20	1±0	2		28±32	4±2		28±25	8
Polytrichum strictum			10	20	9±1					
Sphagnum angustifolium	*SphgAngs*	30±33	32±34	18±19	1±0		13±11	49±42	19±13	58±17
Sphagnum balticum							74			
Sphagnum fuscum		15								
Sphagnum girgensohnii							15			
Sphagnum magellanicum	*SphgMagl*	48		50	15		17±22		3	
Sphagnum russowii	*SphgRuss*	50±57	2		79					

Note: Age classes: AC1, <1 year since thinning; AC2, 4–5 years since thinning; AC3, 14–15 years since thinning. Disturbance classes: DC0, undisturbed; DC1, rut depth <0.2 m; DC2, rut depth >0.2 m. Abbreviation is given to the species presented in Fig. 2.

Table A2. Linear mixed effects analysis of living moss biomass and root production.

	Moss biomass			Root production 0–0.1 m layer			Root production 0.1–0.2 m layer		
	df	*t* value	*p*	df	*t* value	*p*	df	*t* value	*p*
Intercept	60	10.08	0.000	60	11.88	0.000	60	2.66	0.010
AC2	3	−1.53	0.223	3	−1.77	0.175	3	0.45	0.686
AC3	3	−2.54	0.085	3	0.63	0.573	3	0.97	0.402
DC1	60	−6.38	0.000***	60	−5.63	0.000***	60	−0.71	0.478
DC2	60	−8.38	0.000***	60	−4.51	0.000***	60	−0.30	0.769
AC2 × DC1	60	3.85	0.000***	60	5.18	0.000***	60	−0.20	0.842
AC3 × DC1	60	3.05	0.003**	60	2.74	0.008**	60	3.57	0.001**
AC2 × DC2	60	4.71	0.000***	60	0.54	0.594	60	−0.46	0.647
AC3 × DC2	60	5.55	0.000***	60	1.70	0.094	60	2.11	0.039*
Age class	$F_{[2,3]} = 0.9$, $p = 0.49$			$F_{[2,3]} = 6.2$, $p = 0.08$			$F_{[2,3]} = 3.9$, $p = 0.14$		
Disturbance class	$F_{[2,60]} = 25.2$, $p < 0.0001$			$F_{[2,60]} = 18.8$, $p < 0.0001$			$F_{[2,60]} = 1.2$, $p = 0.3$		
Age class × Disturbance class	$F_{[4,60]} = 10.4$, $p < 0.0001$			$F_{[4,60]} = 7.83$, $p < 0.0001$			$F_{[4,60]} = 5$, $p = 0.0015$		

Note: Age classes: AC2, 4–5 years since thinning; AC3, 14–15 years since thinning. Disturbance classes: DC1, rut depth <0.2 m; DC2, rut depth >0.2 m. Significance: *, $p < 0.05$; **, $p < 0.01$; ***, $p < 0.001$.

Table A3. Average microbial biomass carbon (C), and phospholipid fatty acid (PLFA)-based biomass, by age and disturbance classes.

Age class	Disturbance class	Microbial biomass C ($\mu g \cdot g^{-1}$)	$PLFA_{total}$ per dry mass ($nmol \cdot g^{-1}$)	$PLFA_{bact}$ per dry mass ($nmol \cdot g^{-1}$)	$PLFA_{fung}$ per dry mass ($nmol \cdot g^{-1}$)
AC1	DC0	3315 (1551) a	1850 (609) a	769 (278) a	53 (26) a
AC1	DC1	1979 (1231) a	2090 (640) a	812 (238) a	77 (51) a
AC1	DC2	2521 (1296) a	2120 (333) a	860 (146) a	88 (40) a
AC2	DC0	2233 (690) a	1518 (260) a	593 (123) a	72 (38) a
AC2	DC1	2666 (1270) a	2187 (982) a	773 (255) a	145 (139) a
AC2	DC2	2009 (811) a	2010 (1164) a	728 (398) a	113 (81) a
AC3	DC0	2464 (1075) a	1612 (348) a	636 (130) a	73 (49) a
AC3	DC1	3014 (1838) a	1997 (446) a	757 (148) a	139 (114) a
AC3	DC2	2454 (1087) a	1319 (448) a	510 (162) a	66 (49) a

Note: Different lowercase letters in a column indicate significant ($p < 0.05$) differences in interaction effects of age class and disturbance by Tukey pairwise comparison. Age classes: AC1, <1 year since thinning; AC2, 4–5 years since thinning; AC3, 14–15 years since thinning. Disturbance classes: DC0, undisturbed; DC1, rut depth <0.2 m; DC2, rut depth >0.2 m. Standard deviation in parentheses.

Table A4. Linear mixed effects analysis of microbial biomass carbon (C) and phospholipid fatty acid (PLFA)-based biomass.

				PFLA per dry mass								
	C_{mic}			Total			Bacterial			Fungal		
	df	*t* value	*p*	df	*t* value	*p*	df	*t* value	*p*	df	*t* value	*p*
Intercept	59	8.64	0.000	60	10.76	0.000	60	12.31	0.000	60	2.61	0.012
AC2	3	−1.99	0.140	3	−1.37	0.265	3	−1.99	0.141	3	0.65	0.561
AC3	3	−1.56	0.217	3	−0.98	0.400	3	−1.51	0.229	3	0.70	0.535
DC1	59	−2.20	0.032*	60	0.80	0.425	60	0.40	0.689	60	0.72	0.473
DC2	59	−1.31	0.196	60	0.90	0.369	60	0.84	0.405	60	1.05	0.298
AC2 × DC1	59	2.06	0.044*	60	1.02	0.312	60	0.89	0.379	60	1.06	0.296
AC3 × DC1	59	2.19	0.033*	60	0.35	0.731	60	0.51	0.612	60	0.90	0.370
AC2 × DC2	59	0.66	0.509	60	0.53	0.598	60	0.29	0.776	60	0.14	0.886
AC3 × DC2	59	0.92	0.363	60	−1.34	0.187	60	−1.42	0.162	60	−0.90	0.374

Note: Age classes: AC2, 4–5 years since thinning; AC3, 14–15 years since thinning. Disturbance classes: DC1, rut depth <0.2 m; DC2, rut depth >0.2 m. Significance: *, $p < 0.05$; **, $p < 0.01$; ***, $p < 0.001$.

Table A5. Linear mixed effects analysis of carbon dioxide (CO_2) production potential and the residual cellulose mass remaining after 1 year.

				Cellulose remaining after 1 year at:												
	CO_2 production potential			0–5 cm depth			5–10 cm depth			10–20 cm depth			20–30 cm depth			
	df	*t* value	*p*	df	*t* value	*p*	df	*t* value	*p*	df	*t* value	*p*	df	*t* value	*p*	
Intercept	60	6.75	0.000	58	3.87	0.000	58	4.81	0.000	58	7.29	0.000	58	9.09	0.000	
AC2	3	−0.51	0.643	3	−0.73	0.520	3	−0.26	0.815	3	−0.30	0.781	3	−0.28	0.796	
AC3	3	−0.52	0.640	3	−0.45	0.686	3	−0.39	0.722	3	−0.30	0.782	3	−0.96	0.410	
DC1	60	5.33	0.000***	58	−0.45	0.653	58	0.86	0.394	58	1.48	0.144	58	0.98	0.331	
DC2	60	5.61	0.000***	58	0.29	0.770	58	0.02	0.983	58	1.24	0.220	58	0.93	0.358	
AC2 × DC1	60	−3.23	0.002**	58	−0.14	0.889	58	−1.27	0.210	58	−1.08	0.283	58	−0.33	0.742	
AC3 × DC1	60	−1.97	0.054	58	−0.06	0.953	58	−0.72	0.477	58	−1.04	0.303	58	0.19	0.852	
AC2 × DC2	60	0.08	0.933	58	1.11	0.273	58	−0.37	0.715	58	−0.37	0.713	58	−0.23	0.816	
AC3 × DC2	60	−4.51	0.000***	58	1.31	0.195	58	0.72	0.475	58	−0.30	0.764	58	1.03	0.307	
Age class	$F_{[2,3]} = 8.1, p = 0.06$															
Disturbance class	$F_{[2,60]} = 22.6, p < 0.0001$															
Age class × Disturbance class	$F_{[4,60]} = 10, p < 0.0001$															

Note: Age classes: AC2, 4–5 years since thinning; AC3, 14–15 years since thinning. Disturbance classes: DC1, rut depth <0.2 m; DC2, rut depth >0.2 m. Significance: *, $p < 0.05$; **, $p < 0.01$; ***, $p < 0.001$.

Table A6. Linear mixed effects analysis of carbon dioxide (CO_2) and methane (CH_4) concentrations measured in the peat at various depths during 2014.

	CO_2 concentration at:						CH_4 concentration at:					
	5 cm depth			15 cm depth			5 cm depth			15 cm depth		
	df	*t* value	*p*	df	*t* value	*p*	df	*t* value	*p*	df	*t* value	*p*
Intercept	329	0.96	0.336	334	0.85	0.397	329	0.05	0.959	334	0.09	0.925
AC2	3	−0.13	0.908	3	0.00	0.998	3	0.23	0.831	3	0.49	0.657
AC3	3	−0.11	0.919	3	0.10	0.926	3	−0.03	0.976	3	−0.06	0.953
DC1	329	11.22	0.000***	334	12.81	0.000***	329	0.54	0.591	334	2.38	0.018*
DC2	329	15.02	0.000***	334	20.26	0.000***	329	0.77	0.439	334	3.10	0.002**
AC2 × DC1	329	−7.01	0.000***	334	−7.77	0.000***	329	−0.66	0.510	334	−2.31	0.022*
AC3 × DC1	329	−7.46	0.000***	334	−7.90	0.000***	329	−0.36	0.717	334	−1.64	0.102
AC2 × DC2	329	−6.38	0.000***	334	−8.58	0.000***	329	4.36	0.000***	334	2.15	0.033*
AC3 × DC2	329	−8.26	0.000***	334	−12.07	0.000***	329	−0.29	0.772	334	−1.68	0.094
Age class	$F_{[2,3]} = 12.7$, $p = 0.03$			$F_{[2,3]} = 5.3$, $p = 0.10$			$F_{[2,3]} = 0.9$, $p = 0.47$			$F_{[2,3]} = 4$, $p = 0.52$		
Disturbance class	$F_{[2,329]} = 98.2$, $p < 0.0001$			$F_{[2,334]} = 163.1$, $p < 0.0001$			$F_{[2,329]} = 10.3$, $p < 0.0001$			$F_{[2,334]} = 15$, $p < 0.0001$		
Age class × Disturbance class	$F_{[4,329]} = 27.6$, $p < 0.0001$			$F_{[4,334]} = 46.4$, $p < 0.0001$			$F_{[4,329]} = 8$, $p < 0.0001$			$F_{[4,334]} = 6.1$, $p < 0.0001$		

Note: Age classes: AC2, 4–5 years since thinning; AC3, 14–15 years since thinning. Disturbance classes: DC1, rut depth <0.2 m; DC2, rut depth >0.2 m. Significance: *, $p < 0.05$; **, $p < 0.01$; ***, $p < 0.001$.

Table A7. Linear mixed effects analysis of nitrous oxide (N_2O) concentrations measured in the peat at various depths during October 2013.

	N_2O concentration at:					
	5 cm depth			15 cm depth		
	df	*t* value	*p*	df	*t* value	*p*
Intercept	57	3.42	0.001	56	8.11	0.000
AC2	3	−0.14	0.894	3	0.00	0.998
AC3	3	−0.07	0.946	3	0.39	0.725
DC1	57	−0.24	0.810	56	−4.51	0.000***
DC2	57	1.70	0.095	56	−6.56	0.000***
AC2 × DC1	57	0.27	0.788	56	3.81	0.000***
AC3 × DC1	57	0.21	0.832	56	3.00	0.004**
AC2 × DC2	57	−1.53	0.133	56	3.05	0.004**
AC3 × DC2	57	−1.38	0.173	56	3.60	0.001***
Age class	$F_{[2,3]} = 0.5$, $p = 0.64$			$F_{[2,3]} = 2.68$, $p = 0.21$		
Disturbance class	$F_{[2,57]} = 0.2$, $p = 0.82$			$F_{[2,56]} = 16.6$, $p < 0.0001$		
Age class × Disturbance class	$F_{[4,57]} = 0.9$, $p = 0.45$			$F_{[4,56]} = 6$, $p = 0.0004$		

Note: Age classes: AC2, 4–5 years since thinning; AC3, 14–15 years since thinning. Disturbance classes: DC1, rut depth <0.2 m; DC2, rut depth >0.2 m. Significance: *, $p < 0.05$; **, $p < 0.01$; ***, $p < 0.001$.